Inclusion of volatile guests by a tetrapedal host: structure and kinetics

Ayesha Jacobs,*[a] Tanya le Roex,[b] Luigi R. Nassimbeni[a] and Fumio Toda[c]

Received 16th February 2006, Accepted 27th April 2006
First published as an Advance Article on the web 18th May 2006
DOI: 10.1039/b602367n

The host compound tetra(3-hydroxy-3,3-diphenyl-2-propynyl)ethene, **TET**, forms inclusion compounds with acetone, dimethyl sulfoxide, dioxane and pyridine. All the structures were successfully solved in the triclinic space group $P\bar{1}$. We found variable host : guest ratios for the acetone (**TET·ACE**, H : G = 1 : 4), dimethyl sulfoxide (**TET·DMSO**, H : G = 1 : 4) and pyridine compounds (**TET·PYR**, H : G = 1 : 5). Solutions of the host compound and dioxane formed **TET·2DIOX**, H : G = 1 : 2 when left to crystallise at room temperature, whereas **TET·4DIOX**, H : G = 1 : 4 was formed during crystal growth at low temperature. We have correlated the structures with their thermal stabilities and kinetics of desolvation.

Introduction

The concept of multipedal hosts is well established, and MacNicol has reviewed the synthetic strategy of designing hexa-hosts, including the Piedfort idea as well as the more complex spider hosts.[1] These hosts are particularly useful when they contain the diphenylhydroxymethyl moiety, which adds bulk and has the hydroxyl group which acts as a hydrogen bond donor. Thus Weber has synthesised a variety of such compounds where this moiety forms part of roof-shaped hosts,[2] is contained in hosts derived from malic and mandelic acids,[3,4] and in bulky compounds derived from anthracene.[5,6] Toda has employed the same moiety in the synthesis of his wheel-and-axle compounds, which he discovered in 1968, and whose enclathrating abilities have been summarised.[7,8]

We now present the structures, thermal analysis and kinetics of desolvation of five clathrates of the host tetra(3-hydroxy-3,3-diphenyl-2-propynyl)ethene, **TET**, with acetone (**TET·ACE**, H : G = 1 : 4), dimethylsulfoxide (**TET·DMSO**, H : G = 1 : 4), 1,4-dioxane (**TET·2DIOX**, H : G = 1 : 2 and **TET·4DIOX**, H : G = 1 : 4) and pyridine (**TET·PYR**, H : G = 1 : 5). The atomic numbering scheme of the inclusion compounds is given in Scheme 1.

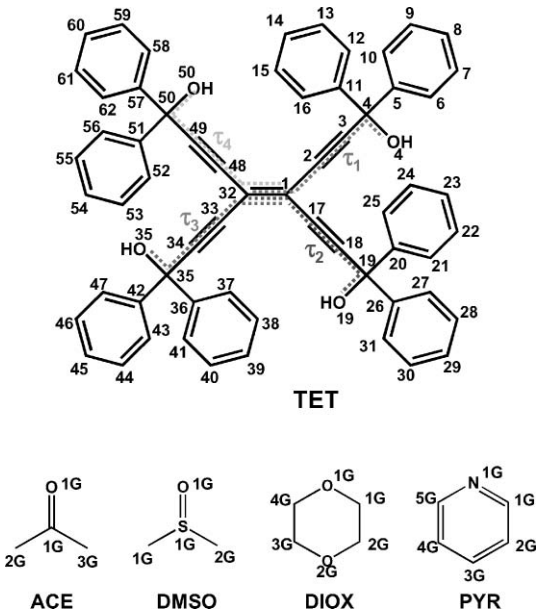

Scheme 1

Experimental

Structure analysis

Crystallographic data, experimental and refinement parameters for all structures are given in Table 1.

Suitable crystals of each of the inclusion compounds were grown by slow evaporation of a solution of the host in the relevant guest at room temperature. The one exception was **TET·4DIOX** which was grown at low temperature (277 K). Cell dimensions for each inclusion compound were established from the intensity data measurements on a Nonius Kappa-CCD diffractometer using graphite-monochromated MoKα radiation, and an Oxford Cryostream cooling system (Oxford Cryostat) was used to control the temperature. The strategy for the data collections was evaluated using the COLLECT[9] software and, for all structures, data were collected using the standard ϕ- and ω-scan techniques, and were scaled and reduced with DENZO-SMN[10] software. The structures were solved by direct methods using SHELX-86[11] and refined by least-squares with SHELX-97[12] refining on F^2. The program X-Seed[13] was used as a graphical interface for structure solution and refinement using SHELX, and the program PovRay, included in the graphical interface X-Seed, was used to produce the packing diagrams.

The mapping of the cavities in which the guest molecules reside was carried out using the program MSRoll.[14] The technique uses a spherical probe which sweeps the volume of the vacant space and estimates its size and topology. The results are sensitive to the radius of the sphere, which has to be chosen with care, in order to yield representative results. This process has been discussed in detail in a recent paper by Barbour.[15]

[a]*Department of Chemistry, Faculty of Applied Sciences, Cape Peninsula University of Technology, P.O. Box 652, Cape Town, 8000, South Africa. E-mail: jacobsa@cput.ac.za; Fax: 27 21 460 3854; Tel: 27 21 460 3167*
[b]*Department of Chemistry, University of Cape Town, Rondebosch, 7701, South Africa*
[c]*Department of Chemistry, Okayama University of Science, Okayama, Japan*

Table 1 Crystal data[a]

Compound	**TET·ACE**	**TET·DMSO**	**TET·2DIOX**	**TET·4DIOX**	**TET·PYR**
Molecular formula	$C_{62}H_{44}O_4{\cdot}4(C_3H_6O)$	$C_{62}H_{44}O_4{\cdot}4(C_2H_6OS)$	$C_{62}H_{44}O_4{\cdot}2(C_4H_8O_2)$	$C_{62}H_{44}O_4{\cdot}4(C_4H_8O_2)$	$C_{62}H_{44}O_4{\cdot}5(C_5H_5N)$
Guest	Acetone	DMSO	1,4-Dioxane	1,4-Dioxane	Pyridine
Host : guest ratio	1 : 4	1 : 4	1 : 2	1 : 4	1 : 5
M/g mol^{-1}	1085.28	1165.48	1029.18	1205.39	1248.47
T/K	113(2)	113(2)	113(2)	173(2)	113(2)
Crystal symmetry	Triclinic	Triclinic	Triclinic	Triclinic	Triclinic
Space group	$P\bar{1}$	$P\bar{1}$	$P\bar{1}$	$P\bar{1}$	$P\bar{1}$
a/Å	13.8204(2)	9.0698(3)	8.6664(2)	9.2037(3)	14.0976(2)
b/Å	13.9878(3)	13.7712(4)	12.6143(2)	12.8577(4)	16.7074(2)
c/Å	16.6312(3)	13.9901(5)	13.1928(3)	14.3892(5)	17.3826(3)
α/°	90.697(1)	71.818(1)	99.167(1)	81.503(1)	63.050(1)
β/°	91.861(1)	71.441(1)	105.288(1)	82.891(1)	87.506(1)
γ/°	109.789(1)	73.849(1)	99.795(1)	79.766(1)	70.950(1)
V/Å^3	3022.7(1)	1542.47(9)	1338.93(5)	1648.97(9)	3423.12(9)
Z	2	1	1	1	2
μ(MoKα)/mm^{-1}	0.076	0.210	0.082	0.081	0.074
Range scanned, θ/°	1.23–27.85	2.42–27.83	1.64–27.91	2.26–27.86	1.72–27.86
Index range	h: −18 to +17, k: −18 to +18, l: −21 to +21	h: −11 to +11, k: −17 to +18, l: −18 to +18	h: −11 to +11, k: −16 to +16, l: −16 to +17	h: −11 to +12, k: −16 to −15, l: −18 to +18	h: −18 to +18, k: −21 to +21, l: −22 to +22
No. reflections collected	25 169	12 296	11 889	14 149	29 704
No. unique reflections	14 069 ($R_{int} = 0.0399$)	6960 ($R_{int} = 0.0437$)	6375 ($R_{int} = 0.0226$)	7684 ($R_{int} = 0.0403$)	16 135 ($R_{int} = 0.0497$)
No. reflections with $I > 2\sigma(I)$	8510	4447	4789	4257	9044
Data/restraints/parameters	14 069/4/763	6960/2/382	6375/2/360	7684/2/409	16 135/7/850
Goodness of fit, S	1.034	1.019	1.052	1.017	1.053
Final R indices ($I > 2\sigma(I)$)	$R_1 = 0.0501$, $wR_2 = 0.1003$	$R_1 = 0.0514$, $wR_2 = 0.1028$	$R_1 = 0.0416$, $wR_2 = 0.0946$	$R_1 = 0.0576$, $wR_2 = 0.1449$	$R_1 = 0.0651$, $wR_2 = 0.1549$
R indices (all data)	$R_1 = 0.1056$, $wR_2 = 0.1166$	$R_1 = 0.1013$, $wR_2 = 0.1187$	$R_1 = 0.0634$, $wR_2 = 0.1034$	$R_1 = 0.1297$, $wR_2 = 0.1704$	$R_1 = 0.1343$, $wR_2 = 0.1811$
Largest diff. peak and hole (e Å^{-3})	0.248; −0.234	0.537; −0.334	0.298; −0.223	0.528; −0.293	0.857; −0.554

[a] CCDC reference numbers 298599–298603. For crystallographic data in CIF or other electronic format see DOI: 10.1039/b602367n

For each structure the non-hydrogen atoms were refined anisotropically, and the aromatic hydrogens on the host and the methyl hydrogens on the guest were placed in geometrically constrained positions with isotropic temperature factors. The hydroxyl hydrogens on the host were located in difference electron density maps and refined with simple O–H bond length constraints.[16] Hydrogens were not placed on disordered atoms.

In the **TET·4DIOX** and **TET·PYR** structures there are some disordered atoms in the guest molecules. In each case the site occupancy factors of the two partial atoms were initially assigned based on peak heights and the temperature factors of the partial atoms forced to refine to the same value. This value was then fixed and the site occupancy factors allowed to refine to give a total site occupancy of one. The refined site occupancy factors were then fixed and the isotropic temperature factors of the two partial atoms were allowed to refine independently.

Thermal analysis and kinetics of desolvation

Thermogravimetry (TG) and differential scanning calorimetry (DSC) were performed on a Perkin–Elmer Pyris 6 system. The TG and DSC experiments were performed over the temperature range 303 K to 523 K at a heating rate of 10 K min^{-1} with a purge of dry nitrogen flowing at 30 ml min^{-1}. The samples were crushed, blotted dry and placed in open ceramic pans for TG and in crimped but vented pans for DSC. Isothermal kinetics was determined by performing TG experiments at a series of constant temperatures.

Results and discussion

The **TET·ACE** structure crystallises in the space group $P\bar{1}$ with $Z = 2$, with the host and four acetone guests all located in general positions. The structure is stabilised by four (host)–O–H···O(guest) hydrogen bonds (average O···O = 2.810(2) Å). All five structures have a very similar hydrogen bonding pattern; the hydrogen bonding of **TET·ACE** is illustrated in Fig. 1 and the metrics of the hydrogen bonds for all the structures are given in Table 2. The packing of the structure, displayed in Fig. 2, is characterised by layers of host molecules lying in the $(\bar{1}02)$ plane and resulting in the formation of three types of cavities in which the acetone guests are located. One of these is a dumbell-shaped cavity, containing four guest molecules, which has a length of approximately 12.5 Å and maximum diameter of approximately 9.0 Å × 4.2 Å. The second type of cavity contains two guest molecules and is approximately 10.4 Å in length with a maximum diameter of 6.9 Å × 4.9 Å, and the third type contains one guest and is approximately 6.9 Å × 5.5 Å × 4.6 Å in size.

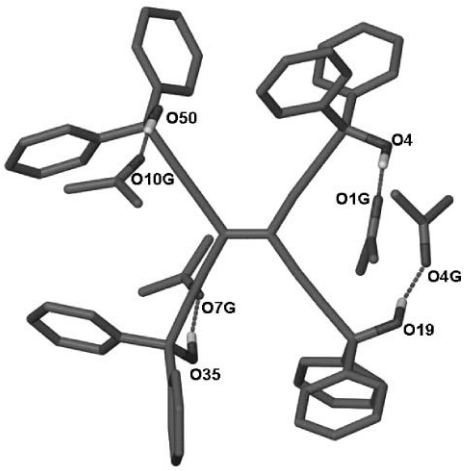

Fig. 1 Molecular structure of **TET·ACE**, showing hydrogen bonding interactions.

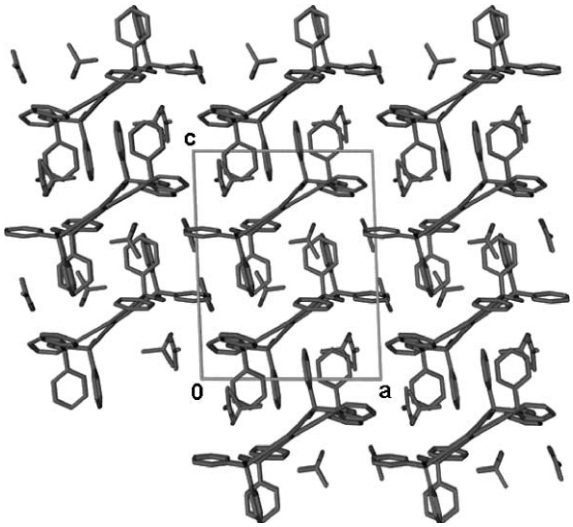

Fig. 2 Packing of **TET·ACE** viewed down [010].

Table 2 Hydrogen bonding details

Inclusion compound	Donor (D)	Acceptor (A)	D···A/Å	D–H/Å	H···A/Å	D–H···A/°
TET·ACE	O4	O1G	2.824(1)	0.955(9)	1.870(9)	176(2)
	O19	O4G	2.830(2)	0.950(9)	1.90(1)	165(2)
	O35	O7G	2.745(1)	0.960(9)	1.80(1)	170(2)
	O50	O10G	2.841(2)	0.960(9)	1.92(1)	161(2)
TET·DMSO	O4	O1G	2.710(2)	0.97(1)	1.74(1)	173(3)
	O19	O3G	2.687(2)	0.97(1)	1.73(1)	168(3)
TET·2DIOX	O4	O1G	2.752(1)	0.959(9)	1.81(1)	165(2)
	O19	O3G	2.806(1)	0.948(9)	1.86(1)	172(2)
TET·4DIOX	O4	O3G	2.795(2)	0.96(1)	1.84(1)	177(3)
	O19	O1G	2.691(2)	0.98(1)	1.75(1)	161(2)
TET·PYR	O4	N1G	2.731(2)	0.99(3)	1.74(3)	176(3)
	O19	N6G	2.740(2)	0.97(3)	1.77(3)	172(3)
	O35	N11G	2.729(2)	0.94(3)	1.80(3)	169(3)
	O50	N16G	2.816(2)	0.94(2)	1.86(1)	176(2)

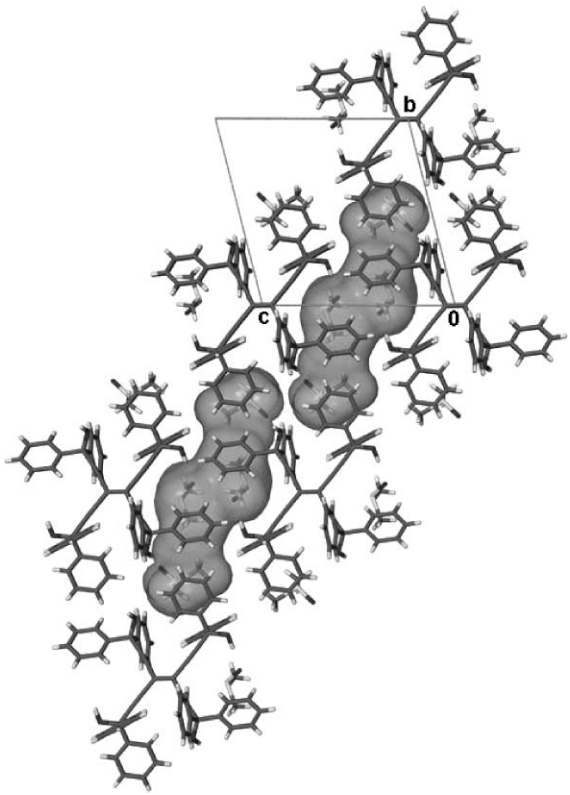

Fig. 3 Packing of **TET·DMSO** viewed along [100] highlighting the cavities containing the guest molecules (cavities calculated using probe size of 1.5 Å).[14]

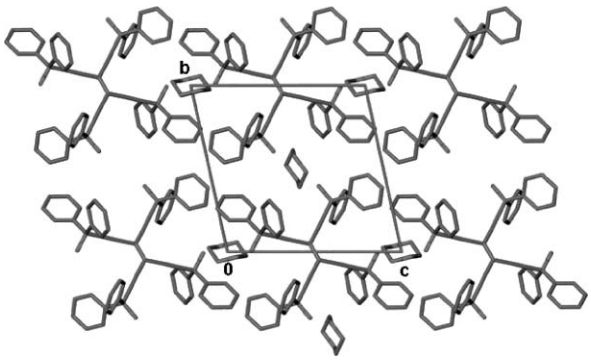

Fig. 4 Packing of **TET·2DIOX** viewed down [100].

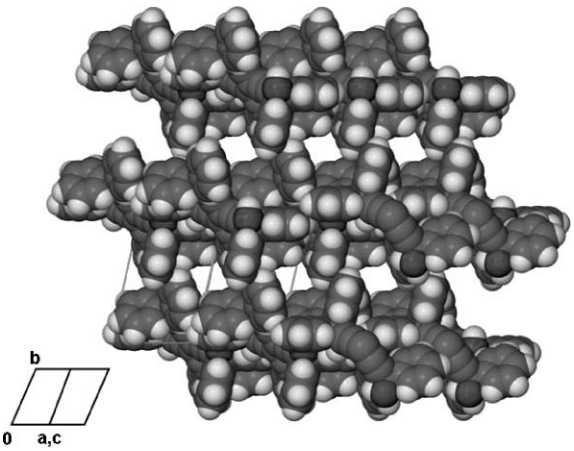

Fig. 5 View down the channels of **TET·4DIOX** along [101] with guest molecules omitted and host molecules represented with van der Waals radii.

The **TET·DMSO** structure crystallises in the space group $P\bar{1}$ with $Z = 1$, and with the host molecule located on a centre of inversion and the guest molecules located in general positions. This structure is also stabilised by intermolecular (host)–O–H···O(guest) hydrogen bonds (average O···O = 2.699(2) Å). In this structure the host molecules stack along [100], resulting in elongated cavities, each of which contain four DMSO guest molecules. These cavities (shown in Fig. 3) are approximately 18.4 Å in length and have a maximum diameter of approximately 8.2 Å × 8.2 Å in the centre, where two guest molecules are located.

The **TET·2DIOX** and **TET·4DIOX** structures both crystallise in the space group $P\bar{1}$ with $Z = 1$, and both structures are stabilised by (host)–O–H...O(guest) hydrogen bonds (average O···O = 2.779(1) Å for **TET·2DIOX** and average O···O = 2.744(2) Å for **TET·4DIOX**). In **TET·2DIOX** the host and guest molecules are located on centres of inversion. In the packing of the structure, displayed in Fig. 4, the host molecules stack along [100], resulting in two rows of cavities in the unit cell along the same direction, in which the guests are located. These two types of cavities have dimensions of 7.5 Å × 7.3 Å × 6.9 Å and 7.6 Å × 7.6 Å × 4.3 Å, with all cavities containing one guest molecule.

In **TET·4DIOX** the host molecule and two of the four guest molecules are located on centres of inversion, and the remaining two guest molecules located in general positions. The crystal packing displays layers of host molecules in the (101) plane, resulting in the formation of undulating channels along [$\bar{1}$01], which can be seen in Fig. 5, in which the 1,4-dioxane guests are located. The diameter of these channels remains fairly constant at approximately 6.1 Å × 4.8 Å.

The **TET·PYR** structure crystallises in the space group $P\bar{1}$ with $Z = 1$, and with both the host and guest molecules located in general positions. In this structure four of the guest molecules are hydrogen bonded to the host molecule *via* intermolecular (host)–O–H···O(guest) hydrogen bonds (average O···O = 2.754(2) Å), while the fifth guest molecule is not involved in hydrogen bonding. This guest molecule is disordered over two positions, with both partial molecules sharing a common nitrogen atom. One of the hydrogen-bonded guest molecules also has two carbon atoms disordered over two positions. In this structure the host molecules pack in layers similar to those observed in **TET·ACE**, in this case parallel to the (101) plane, resulting in narrow channels along [100] which link a series of cavities, each containing five guest molecules. These cavities (illustrated in Fig. 6) have an irregular shape and are restricted by the channel diameter, which is approximately 3.6 Å × 5.9 Å.

The pseudotorsion angles defining the position of each hydroxyl group relative to the central ethene bond of the host molecule are displayed in Scheme 1, and Table 3 compares these angles in each of the inclusion compounds, as well as with those found in the inclusion compounds of the same host with cyclohexanone[17] (**TET·CHO**) and dimethyl acetamide[18] (**TET·DMA**). It can be seen that in **TET·ACE** and **TET·PYR**, on one side of the central

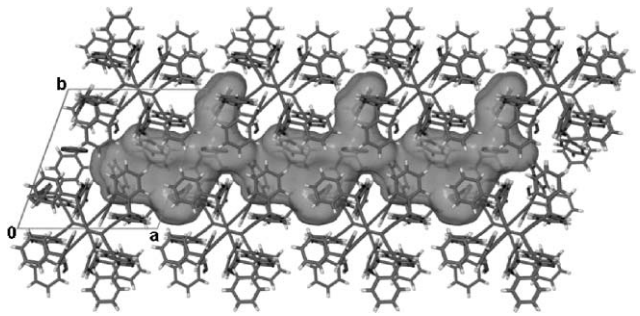

Fig. 6 Packing of **TET·PYR** viewed along [001], highlighting the cavities containing the guest molecules (cavities calculated using probe size of 1.5 Å).[14]

Table 3 Pseudotorsion angles[a] describing host conformation

Inclusion compound	τ_1/°	τ_2/°	τ_3/°	τ_4/°
TET·ACE	165.6	170.0	−47.5	−46.9
TET·DMSO	−176.3	42.5	—	—
TET·2DIOX	178.6	28.1	—	—
TET·4DIOX	−168.4	−64.8	—	—
TET·PYR	176.9	165.0	−55.1	−40.2
TET·CHO[16]	−176.9(3)	45.1(3)	50.5(3)	179.7(3)
TET·DMA[17]	8.7(3)	20.3(3)	—	—

[a] *e.g.* O4–C4–C1–C32

double bond there is one hydroxyl group pointing upwards and one downwards, while on the other side of the double bond the two hydroxyl groups are relatively flat, with the O–H vector pointing away from the central double bond in each case. This conformation of the host is very similar to that observed in the inclusion compound with cyclohexanone. The conformation of the host molecules in **TET·DMSO**, **TET·2DIOX** and **TET·4DIOX** are very similar. On one side of the double bond there is one hydroxyl group pointing upwards and one which is relatively flat, while on the other side there is one pointing downwards and one which is relatively flat. The two which are relatively flat are not adjacent to each other and point away from the central double bond, while the other two have the O–H vector pointing inwards towards the central double bond. The conformation of the host in **TET·DMA** is different to those described above, with all O–H vectors directed inwards towards the central double bond.

The results of the thermal analysis experiments are given in Table 4. The TG results confirmed host : guest ratios of 1 : 4 for **TET·ACE**, **TET·DMSO** and **TET·4DIOX** and a host : guest ratio of 1 : 5 for **TET·PYR**. Overall, there is good agreement between the calculated and experimental results. For the **TET·ACE** compound the TG curve shows a single desolvation step corresponding to the loss of guest. The corresponding DSC trace exhibits an endotherm due to guest desorption ($T_{on} = 333$ K) followed by the endotherm due to the melt of the host immediately followed by rapid host decomposition. The **TET·DMSO** compound decomposes *via* a multistep pathway. TG analysis of the individual steps indicated an initial loss of one guest followed by the loss of two guests and finally the release of the last guest molecule. The DSC curves show the endotherms corresponding to the first two guest desorptions. The TG curve for the **TET·4DIOX** compound shows two steps, with each individual step corresponding to the loss of two guests.

This result is confirmed by the DSC curve, which indicates two endotherms due to guest desorption followed by host decomposition. The TG trace for **TET·PYR** also shows two steps, the first step corresponding to the loss of three guests and the second step corresponding to release of the last two guest molecules. The DSC curve is rather complex, with an initial endotherm at $T_{on} =$ 370.0 K.

We have employed the parameter $T_{on} - T_b$ as a measure of the stability of a host–guest compound. In our case, for **TET·DMSO** the two endotherms have values of $T_{on} - T_b$ of −126.5 K and −68.4 K respectively. These values are summarised in Table 4. On this basis the **TET·4DIOX** clathrate is the more stable, but such comparisons have limited value when the guests have such large differences in their normal boiling points.

Kinetics of desolvation were determined for the **TET·ACE** inclusion compound by performing a series of isothermal TG experiments between 308 K and 328 K. The resultant mass–time curves were deceleratory and fitted the first order rate law (F1): $[-\ln(1 - \alpha)] = kt$ where α is the extent of the reaction and k is the rate constant.[19] This equation fitted the first order law over a wide range ($\alpha = 0.05$ to 0.98) with high coefficients of correlation, typically 0.9979. A plot of ln k *vs.* $1/T$ (Fig. 7) gave a linear result. An activation energy of 121 kJ mol^{-1} for the desolvation reaction was obtained from the negative slope due to the relation $-E_a/R =$ slope, where E_a is the activation energy and R is the universal gas constant. This result compares favourably with the activation energy obtained for the desolvation

Table 4 Thermal analysis data

Inclusion compound		**TET·ACE**	**TET·DMSO**	**TET·4DIOX**	**TET·PYR**
H : G ratio		1 : 4	1 : 4	1 : 4	1 : 5
TG	(calc % mass loss)	21.4	26.8	29.2	31.7
	(exp % mass loss)	20.3	26.9	29.1	31.6
DSC	T_{on}/K	333.0	335.5	399.6	370.0
	T_{on}/K	—	393.6	444.7	—
	T_{on}/K	477.5	—	—	—
T_b/K[a]		329	462	374	388
$T_{on} - T_b$		4	−126.5	25.6	−18.3
			−68.4	70.7	

[a] Normal boiling point.

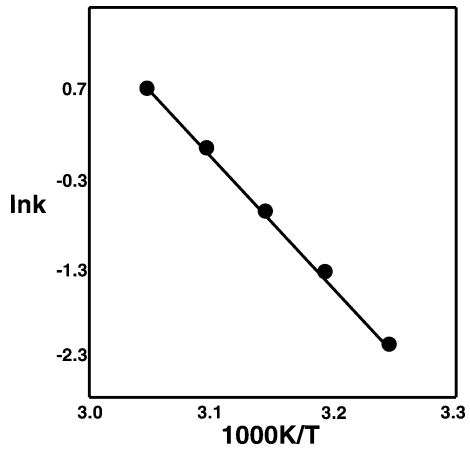

Fig. 7 Arrhenius plot for the desolvation of **TET·ACE**.

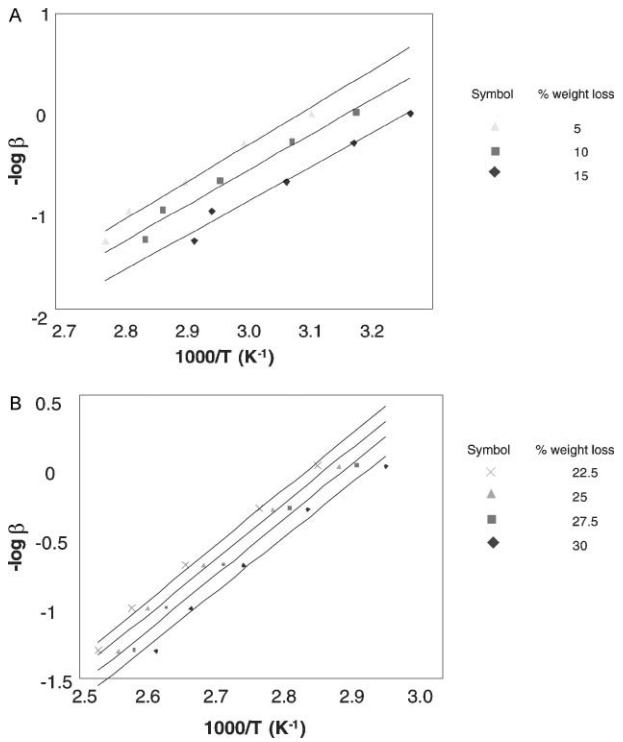

Fig. 8 Plot of $-\log\beta$ *vs.* $1/T$ for **TET·PYR** indicating (A) step one and (B) step two.

of the *N*,*N*-dimethylacetamide (DMA) clathrate,[18] which has an activation energy of 117 kJ mol^{-1}. In both instances the guests are held in cavities with similar hydrogen bond parameters. Similar results were also obtained for the desorption of DMA from its inclusion compound with the host (H) = 9,9′-(biphenyl-4,4′-diyl)bis(fluoren-9-ol). This compound, H·4DMA, decomposes in two steps, each involving loss of two DMA guests. The kinetics yielded activation energies of 79.1 kJ mol^{-1} and 115.4 kJ mol^{-1} for the first and second steps respectively.[20]

A non-isothermal kinetics method was used to study the desolvation of **TET·PYR**. Ideally, isothermal methods are preferred, but in this case the two steps in the TG curve could not be separated even at very low temperatures. Thus the method of Flynn and Wall[21] was employed to determine the activation energy. A series of TG experiments over a temperature range of 303–403 K were performed at heating rates of 1, 2, 5, 10 and 20 K min^{-1}. The TG curves were analysed at different stages of decomposition ranging from 5% to 15% for the first step and 22.5% to 30% for the second step. By convention the corresponding negative log of the heating rate (β) *vs.* reciprocal temperature were plotted (Fig. 8). This allowed us to calculate the activation energy ranges for the two steps. The results for both steps were similar, with the activation energy range for step one being 70–77 kJ mol^{-1} and for step two being 74–76 kJ mol^{-1}. The lower activation energy for **TET·PYR** than for **TET·ACE** is consistent with the lower $T_{on} - T_b$ value obtained for **TET·PYR** and the observation that for **TET·ACE** the guests are trapped in cavities, whereas for **TET·PYR** the guests lie in narrow channels.

References

1 D. D. MacNicol, 'Solid State Supramolecular Chemistry: Crystal Engineering', in: *Comprehensive Supramolecular Chemistry (Vol.6)*, ed. F. Toda and R. Bishop, Pergamon, Oxford, 1996.
2 I. Csöregh, E. Weber and T. Hens, *J. Inclusion Phenom. Macrocyclic Chem.*, 2000, **38**, 397.
3 E. Weber, A. Zaumüller, W. Seichter and M. Czugler, *Supramol. Chem.*, 1997, **8**, 351.
4 E. Weber, O. Hager, C. Foces-Foces and A. L. Llama-Saiz, *Supramol. Chem.*, 1998, **9**, 85.
5 E. Weber, T. Hens, Q. Li and T. C. W. Mak, *Eur. J. Org. Chem.*, 1999, 1115.
6 E. Weber, T. Hens, T. Brehmer and I. Csöregh, *J. Chem. Soc., Perkin Trans. 2*, 2000, 235.
7 F. Toda and K. Akagi, *Tetrahedron Lett.*, 1968, 3695.
8 F. Toda, in: *Inclusion Compounds (Vol. 4)*, ed. J. L. Atwood, J. E. D. Davies and D. D. MacNicol, Oxford University Press, Oxford, 1991, ch. 4.
9 *COLLECT, Data collection software*, Nonius, Delft, The Netherlands, 1999.
10 Z. Otwinowski and W. Minor, in: 'Macromolecular Crystallography, Part A' (*Methods in Enzymology, Vol. 276*), ed. C. W. Carter and R. M. Sweet, Academic Press, New York, 1997, pp. 307–326.
11 G. M. Sheldrick, in *Crystallographic Computing*, ed. G. M. Sheldrick, C. Kruger and P. Goddard, Oxford University Press, Oxford, 1985, vol. 3, p. 175.
12 G. M. Sheldrick, *SHELX-97, Program for Crystal Structure Determination*, University of Göttingen, Germany, 1997.
13 L. J. Barbour, *J. Supramol. Chem.*, 2001, **1**, 189; J. L. Atwood and L. J. Barbour, *Cryst. Growth Des.*, 2003, **3**, 3.
14 M. L. Connolly, *Science*, 1983, **221**, 709–713; M. L. Connolly, *J. Am. Chem. Soc.*, 1985, **107**, 1118–1124.
15 L. J. Barbour, *Chem. Commun.*, 2006, 1163.
16 P. Schuster, G. Zundel and C. Sandorfy, *The Hydrogen Bond: Recent Developments in Theory and Experiments, Vol. 3: Dynamics, Thermodynamics and Special Systems*, 1976, American Elsevier Pub. Co., Amsterdam.
17 S. A. Bourne, K. L. Gifford-Nash and F. Toda, *J. Chem. Crystallogr.*, 1999, **29**, 261.
18 S. A. Bourne, K. L. Gifford-Nash and F. Toda, *J. Mol. Struct.*, 1999, **474**, 223.
19 M. E. Brown, *Introduction to Thermal Analysis*, 1988, Chapman and Hall, New York, ch. 13.
20 M. R. Caira, T. Le Roex, L. R. Nassimbeni, J. A. Ripmeester and E. Weber, *Org. Biomol. Chem.*, 2004, **2**, 2299–2304.
21 J. H. Flynn and L. H. Wall, *J. Polym. Sci., Part B: Polym. Lett.*, 1966, **4**, 323.